INTERNATIONAL JOURNAL OF CLIMATOLOGY
Int. J. Climatol. **37** (Suppl.1): 1105–1117 (2017)
Published online 17 April 2017 in Wiley Online Library
(wileyonlinelibrary.com) DOI: 10.1002/joc.5069

RMetS
Royal Meteorological Society

Uncertainty assessment for climate change impact on intense precipitation: how many model runs do we need?

Parisa Hosseinzadehtalaei,[a]* Hossein Tabari[a] and Patrick Willems[a,b]
[a] *Hydraulics Division, Department of Civil Engineering, KU Leuven, Belgium*
[b] *Department of Hydrology and Hydraulic Engineering, Vrije Universiteit Brussel, Belgium*

ABSTRACT: Precipitation projections are typically obtained from general circulation model (GCM) outputs under different future scenarios, then downscaled for hydrological applications to a watershed or site-specific scale. However, uncertainties in projections are known to be present and need to be quantified. Although GCMs are commonly considered the major contributor of uncertainty for hydrological impact assessment of climate change, other uncertainty sources must be taken into account for a thorough understanding of the hydrological impact. This study investigates uncertainties related to GCMs, GCM initial conditions and representative concentration pathways (RCPs) and their sensitivity to the selection of GCM runs in order to quantify the impact of climate change on extreme precipitation and intensity/duration/frequency statistics. The results from a large ensemble of 140 CMIP5 GCM runs including 15 GCMs, 3–10 GCM initial conditions and 4 RCPs are analysed. Albeit the choice of GCM is the major contributor (up to 65% for some cases) to intense precipitation change uncertainty for all return periods (1 year, 10 years) and aggregation levels (1-, 5-, 10-, 15- and 30-day), uncertainties related to the GCM initial conditions and RCPs of up to 38 and 23%, respectively, are found in some cases. The sensitivity analysis reveals that the GCM, RCP and GCM initial condition uncertainties are greatly influenced by the set of climate model runs considered, especially for more extreme precipitation at finer time scales.

KEY WORDS extreme precipitation; CMIP5 GCM; ensemble size; uncertainty analysis; sensitivity analysis

Received 2 September 2016; Revised 30 January 2017; Accepted 28 February 2017

1. Introduction

Climate change projections indicate that an increase in the intensity and frequency of precipitation extremes is more likely in the face of climate warming, especially by the end of the 21st century [Intergovernmental Panel on Climate Change (IPCC), 2012, 2013; Willems *et al.*, 2012a; Liew *et al.*, 2014; O'Gorman, 2015; Sunyer *et al.*, 2015; Wu *et al.*, 2015; Tabari *et al.*, 2016a]. To specify extreme precipitation to prepare the design guidelines for water infrastructure, the most popular method is to find relationships between precipitation intensity, duration and frequency represented as intensity–duration–frequency (IDF) curves. These curves are important tools for hydrological planning and structural design associated with water resource management. The infrastructure design is sensitive to potential changes in extreme precipitation characteristics under climate change, and non-stationary climate conditions will increase the probability of failure of the structures designed by applying the current IDF curves. Therefore, updating the existing IDF curves by taking climate change impact on the design precipitation into consideration will greatly facilitate damage limitation (Willems *et al.*, 2012b). The expected changes in IDF statistics under climate change in different parts of the world further emphasize the urgency of this requirement (Peck *et al.*, 2012; Willems *et al.*, 2012b; Cheng and AghaKouchak, 2014; De Paola *et al.*, 2014; Modesto Gonzalez Pereira *et al.*, 2014; Latifa *et al.*, 2015; Tabari *et al.*, 2016b).

Global climate models (GCMs) are the main tools for assessing the impact of climate change (Randall *et al.*, 2007; Chen *et al.*, 2014; Liu *et al.*, 2014; Alfieri *et al.*, 2015; Panday *et al.*, 2015). Recently, GCMs provided by the Coupled Model Intercomparison Project Phase 5 (CMIP5) have been widely applied in the climate change analysis (Kharin *et al.*, 2013; Yin *et al.*, 2013; Liu *et al.*, 2014; Rana *et al.*, 2014; Tabari *et al.*, 2015; Hosseinzadehtalaei *et al.*, 2016; Janssen *et al.*, 2016). The CMIP5 provides a set of coordinated climate model simulations for the IPCC 5th Assessment report (AR5). Compared to the earlier phase (CMIP3), CMIP5 simulations represent a larger number of more complex models with higher spatial resolution and an improvement in models' physics, leading to incorporation of more progressed behaviour of land use changes and better demonstration of the mean condition of atmospheric variables including surface temperature and

* Correspondence to: P. Hosseinzadehtalaei, Hydraulics Division, Department of Civil Engineering, KU Leuven, Kasteelpark Arenberg 40, BE-3001 Leuven, Belgium. E-mail: parisa.hosseinzadehtalaei@kuleuven.be

Table 1. Summary of 15 climate models from CMIP5 used in this study.

Model	Spatial resolution (Lon × Lat)	Number of runs				
		His.	RCP2.6	RCP4.5	RCP6.0	RCP8.5
BCC-CSM1.1	~2.81° × 2.79°	1	1	1	1	1
BCC-CSM1.1(m)	~2.81° × 2.79°	1	1	1	1	1
CCSM4	1.25° × 0.94°	3	3	3	3	3
CSIRO-Mk3.6.0	1.875° × 1.875°	10	10	10	10	10
GFDL-CM3	2.5° × 2°	1	1	1	1	1
GFDL-ESM2G	2° × 2.02°	1	1	1	1	1
GFDL-ESM2M	2.5° × 2°	1	1	1	1	1
HadGEM2-ES	1.875° × 1.25°	3	3	3	3	3
IPSL-CM5A-LR	3.75° × 1.895°	1	1	1	1	1
IPSL-CM5A-MR	2.5° × 1.27°	1	1	1	1	1
MIROC-ESM	~2.8° × 2.8°	1	1	1	1	1
MIROC-ESM-CHEM	~2.8° × 2.8°	1	1	1	1	1
MIROC5	1.40° × 1.40°	1	1	1	1	1
MRI-CGCM3	1.125° × 1.121°	1	1	1	1	1
NorESM1-M	2.5° × 1.9°	1	1	1	1	1

precipitation (Hawkins and Sutton, 2009; Meehl and Bony, 2011; Taylor *et al.*, 2012; Knutti and Sedláček, 2013; Sierra *et al.*, 2015). However, the projections of future climate conditions using the GCM simulations are subject to uncertainties with distinct sources due to different future emission/concentration scenarios, parameterization and structure of GCMs, boundary and initial conditions (Min *et al.*, 2007; Liepert and Previdi, 2012; Brekke and Barsugli, 2013; Strobach and Bel, 2015). The uncertainty is larger for the future projections of climate extremes (Ahmed *et al.*, 2013; Horton *et al.*, 2015; Ning *et al.*, 2015; Ning and Bradley, 2016), due to the difficulty in the modelling of extremes. Quantification of the uncertainty is one of the main steps in identifying the adaptation measures for water resources management in the face of climate change. Therefore, the relative magnitude of each of the uncertainty sources might be defined to achieve the minimal uncertainties to extreme precipitation and construction of future IDF curves.

The application of multi-model ensembles to quantify the projection uncertainty of climate change has recently increased in hydrological studies (Minville *et al.*, 2008; Chen *et al.*, 2011; Hughes *et al.*, 2011; Kingston *et al.*, 2011; Dessu and Melesse, 2013; Mandal *et al.*, 2016). The larger the ensemble size of independent climate models considered, the better the quantification of climate change uncertainty would be. Independent and most accurate climate models for each region can be selected using envelope and past-performance approaches (Cannon, 2015; Lutz *et al.*, 2016; Mendlik and Gobiet, 2016). Nevertheless, maximizing the model diversity to cover the total uncertainty through a larger ensemble of representative climate models places a greater demand on computational resources (Ferro *et al.*, 2012). Due to the expense of larger ensembles of simulations and resource constraints, a perennial question is how sensitive are the uncertainty results to the size of the climate model ensemble and the selected climate model runs. This research question is addressed in this study by performing a sensitivity analysis on how changes in ensemble size affect the magnitude of uncertainty for intense precipitation changes.

The impact of climate change on intense precipitation and IDF curves has been investigated before in several studies (e.g. Mailhot *et al.*, 2007; Madsen *et al.*, 2009; Willems *et al.*, 2012b; Yilmaz *et al.*, 2014; Kim *et al.*, 2015). Such impact analysis is complemented in this study with a thorough investigation of the uncertainties. This is done for IDF statistics and curves under projections of climate change scenarios provided by the CMIP5 GCMs for different return periods and durations, for central Belgium. The magnitude of the uncertainty in the future precipitation extremes and IDF statistics related to the choice of the GCMs, RCPs and initial conditions are assessed. This is done starting from a large ensemble of GCM runs available in the CMIP5 database. The sensitivity of each of the three uncertainty contributors to the GCM ensemble size is also analysed.

2. Methodology

2.1. Data

Climate simulations for control and scenario periods with different future scenarios have been provided by CMIP5 data sources. In this study, daily precipitation data from 15 GCMs are used, from 1961 to 1990 for the control period and from 2071 to 2100 for the scenario period. The GCMs having precipitation data for all RCPs at the time of analysis were selected. Table 1 presents the CMIP5 model simulations considered in this study. Four future greenhouse gas scenarios in the form of the standard representative concentration pathways (RCPs) are used, including RCP2.6, RCP4.5, RCP6.0 and RCP8.5. These scenarios represent a range from low to high levels of greenhouse gas concentrations by the year 2100. For each GCM, just one run is selected which is the first initial condition. However, for considering the uncertainty in the GCM initial

conditions 10 available runs of CSIRO-Mk3.6.0 GCM are also evaluated. In addition, three runs of CCSM4 and HadGEM2-ES GCMs are also used. The preliminary analysis showed that the first run of the MIROC5 model was an extreme outlier. Such deficiency of the model was reported in the literature (e.g. Sillmann *et al.*, 2013a, 2013b). As this extreme outlier will overshadow the results and regarding the non-selective choice of the GCMs and their respective runs in this study, we used the second run of MIROC5 for further analysis. In total, 140 CMIP5 GCMs runs are analysed. The GCM simulations are evaluated relative to observation data at Uccle station (Brussels). This station is operated by the Royal Meteorological Institute of Belgium and has high quality, long rainfall records. Next to the point observations, gridded daily precipitation values from the E-OBS data set (v12.0, Haylock *et al.*, 2008) from the European Climate Assessment and Data (ECA&D) for 0.5° and 0.25° spatial resolutions are used. These gridded data are aggregated to larger pixels of 111 and 445 km for comparison with the gridded CMIP5 GCM results at similar spatial resolutions.

2.2. Construction of IDF curves and associated uncertainties

The IDF curves are created for the control and scenario periods based on the outputs of the CMIP5 GCMs. This is done by using statistical extreme value analysis. Willems (2000) has set up the IDF curves for Belgium on the basis of peak-over-threshold (POT) extreme value statistics after calibration of two-component exponential distributions. The IDF construction method uses the POT approach by which a more rational selection of extreme events is possible, instead of considering only one event per year in the annual maxima method. The distributions are calibrated by weighted regression in the exponential quantile plot to extract nearly independent precipitation intensity extremes from the time series by means of independence criteria. The return period for the two-component exponential distribution is computed for the POT-selected independent extremes, x, by:

$$T = \frac{n}{t(p_a\left(1 - G_a\left(x\right)\right) + \left(1 - p_a\right)\left(1 - G_b\left(x\right)\right)} \quad (1)$$

where T is the return period in years, n is the total length of precipitation time series in years, t is the observed order of the threshold level above which the distribution is considered, p_a is the proportion of population a, and $G_a(x)$ and $G_b(x)$ are two different exponential distribution functions for subpopulations a and b. The two subpopulations are hypothesized to be related to convective and frontal types of rain storms. $G_a(x)$ and $G_b(x)$ are computed as:

$$G_a\left(x\right) = 1 - \exp\left(-\frac{x - x_t}{\beta_a}\right) \quad (2)$$

$$G_b\left(x\right) = 1 - \exp\left(-\frac{x - x_t}{\beta_b}\right) \quad (3)$$

where β is the distribution parameter and x_t is the optimal threshold.

Following this method, IDF curves are constructed for the simulations of CMIP5 GCMs. Once the IDF curves are created for the control and scenario periods, future downscaled IDF curves are constructed by applying climate change factors to the existing IDF statistics driven from station observations on the basis of a quantile perturbation downscaling method:

$$\mathrm{IDF}_F\left(D,T\right) = \mathrm{IDF}_O\left(D,T\right) \times \frac{\mathrm{IDF}_S\left(D,T\right)}{\mathrm{IDF}_C\left(D,T\right)}$$
$$D = 1,\ 5,\ 10,\ 15,\ 30 \text{ days } T = 1,\ 10 \text{ years} \quad (4)$$

where $\mathrm{IDF}_S(D,T)$, $\mathrm{IDF}_C(D,T)$, $\mathrm{IDF}_O(D,T)$ and $\mathrm{IDF}_F(D,T)$ are the extreme precipitation intensities of return period T and duration D for the scenario and control runs, the observations, and the perturbed observations representing the future climate conditions, respectively. The ratio $\frac{\mathrm{IDF}_S(D,T)}{\mathrm{IDF}_C(D,T)}$ is the climate change factor defined as the ratio between the precipitation intensity for the scenario period and the corresponding intensity in the control period for the same return period and aggregation level. The applicability of the quantile perturbation method has been demonstrated and tested for extreme precipitation downscaling (Willems, 2013; Maurer and Pierce, 2014; Ntegeka *et al.*, 2014; Cannon *et al.*, 2015; Maraun, 2016). For a detailed explanation of the quantile perturbation downscaling method applied in this study, see Willems (2013) and Ntegeka *et al.* (2014).

As the second objective of this study, different sources of uncertainties for the projected change in extreme precipitation and IDF statistics due to GCMs, GCM initial conditions and RCPs are quantified. To determine the GCM uncertainty, we calculate the scenario range in the extreme precipitation statistics for the different GCM runs after averaging these statistics over different RCPs and different runs of the CSIRO-Mk3.6.0 model. The scenario range is computed as the difference between the high and low climate scenarios defined based on the 95% confidence interval limits. Similarly, to estimate RCP uncertainty we average different runs of the CSIRO-Mk3.6.0 model and different GCMs within each RCP and then calculate the scenario range between the four RCPs. For computing the uncertainty associated with the GCM initial conditions, the scenario range between the different runs of the CSIRO-Mk3.6.0 model is calculated after averaging over the different RCPs. The above-mentioned uncertainty analysis for each of the three components is repeated for different ensemble sizes of GCMs, RCPs and GCM initial conditions to analyse the sensitivity of the uncertainty rate to the ensemble size.

3. Results and discussion

3.1. GCM-based IDF curves

The general validation of the CMIP5 GCM ensemble-based current IDF curves compared to those driven from the observations for different return periods (1 year and 10 years) and aggregation levels (1-, 5-, 10-,

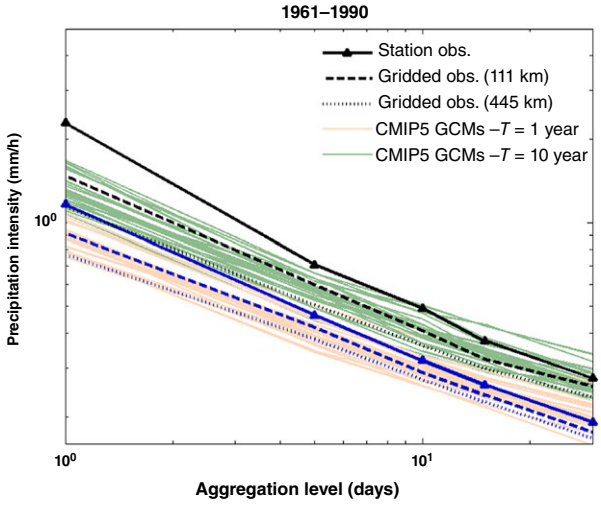

Figure 1. Validation of precipitation IDF curves derived from CMIP5 runs based on Uccle observations for the historical period (1961–1990) (observation lines for the 1- and 10-year return periods are shown in blue and black colours, respectively).

15- and 30- day) is shown in Figure 1. As shown, all GCMs have a tendency to underestimate design precipitation for different return periods and aggregation levels compared with the station observations which are typically used for hydraulic design. This underestimation is more obvious for the smaller (i.e. daily) time scales. This bias is a well-known feature of GCMs, and may be at least partly explained by the spatial scale difference between point observations and gridded model results (Willems *et al.*, 2012a; Sunyer *et al.*, 2013a; Rana *et al.*, 2014). When the GCM-driven IDF curves are compared with those from the gridded observations, the systematic deviation reduces, which confirms that the underestimation in comparison with the point observations is due to the spatial scale difference. After comparison with the gridded observations, however, still overestimations and underestimations are detectable for individual model runs.

To construct future downscaled IDF curves based on the quantile perturbation downscaling method, change factors need to be calculated. These change factors are computed for design precipitation after consideration of intensity, duration and frequency aspects. Figure 2 shows the change factors for precipitation IDF statistics of different return periods and durations under different RCP scenarios. The results indicate an intensification of extreme precipitation for almost all durations and return periods. This intensification is more pronounced for more extreme precipitation and smaller time scales. As expected, the increment in extreme precipitation increases from RCP2.6 to RCP8.5. Generally, the intense precipitation and IDF statistics will increase up to around 64% by the end of this century. This projected increase in extreme precipitation for Belgium based on the CMIP5 GCM results is higher than the increase obtained in earlier studies for the same location. Willems and Vrac (2011) projected an increase of up to about 30% using a set of 17 ensemble runs from the ECHAM5 GCM, whereas Willems (2013) obtained a maximum increase of 50% using a large ensemble of older generation (CMIP3) RCM and GCM runs. In Figure 2, the highest changes go up to about 64% for a return period of 10 years and the smallest duration (1 day) considered under the RCP8.5 scenario.

In the framework of the quantile perturbation downscaling method, the change factors were applied on the Uccle observations to obtain future IDF curves as shown in Figure 3. For all RCPs, the precipitation intensities for the future IDF curves are larger than those for the existing curves, with more intensification for the more extreme RCP scenario (i.e. RCP8.5). The inadequacy of the existing IDF curves, as a result of intense precipitation amplification especially for longer recurrence interval and higher temporal resolution, increases the water infrastructure failure risks for the future.

3.2. Climate change signal uncertainty for IDF relationships and its sensitivity to selected GCM runs

The total uncertainty in the projection of design precipitation in the form of IDF curves is decomposed into the three uncertainty sources addressed in this article, and the influence of the choice of the GCMs, RCPs and GCM initial conditions on the projection of design precipitation is evaluated. The design precipitation changes over different RCPs, GCMs and GCM initial conditions are shown in Figure 4. In general, the changes in the future extreme precipitation projections increase from RCP2.6 to RCP8.5, which is trivial given the higher hypothesized increase in greenhouse gas concentrations in the more extreme scenarios. The uncertainty in the changes of extreme precipitation due to different RCPs is generally large, ranging from 8% in RCP2.6 to 19–21% in RCP8.5. The difference is larger for more intense precipitation, as is shown for a return period of 10 years in comparison to the 1-year return period. Projected change difference over GCMs shows that the change amount varies substantially across the various GCMs. The related changes vary from 1.39% for the BCC-CSM1.1 GCM for the 10-year daily intensity to 44% for the GFDL-CM3 for the same return period and time scale. The NorESM1-M model is the only GCM which shows a negative change for the 10-year return period. Similar to GCMs and RCPs, the projected changes vary considerably over different CSIRO-MK3-6-0 GCM initial conditions, with run 7 for 10-year return period showing the lowest change of 1.8% and run 1 showing the highest change of 35% for the same return period (Figure 4). Generally, it is found from the results that the magnitude of changes in design precipitation at different return periods and durations is very sensitive to the choice of any of the three considered variates, GCMs, RCPs and GCM initial conditions.

Percentage of total variation in change factors for design precipitation explained by GCM, RCP and GCM initial condition uncertainties for the selected return periods and durations is shown in Figure 5. As can be seen, GCM uncertainty is dominant throughout different durations and return periods: always larger than 49% and as

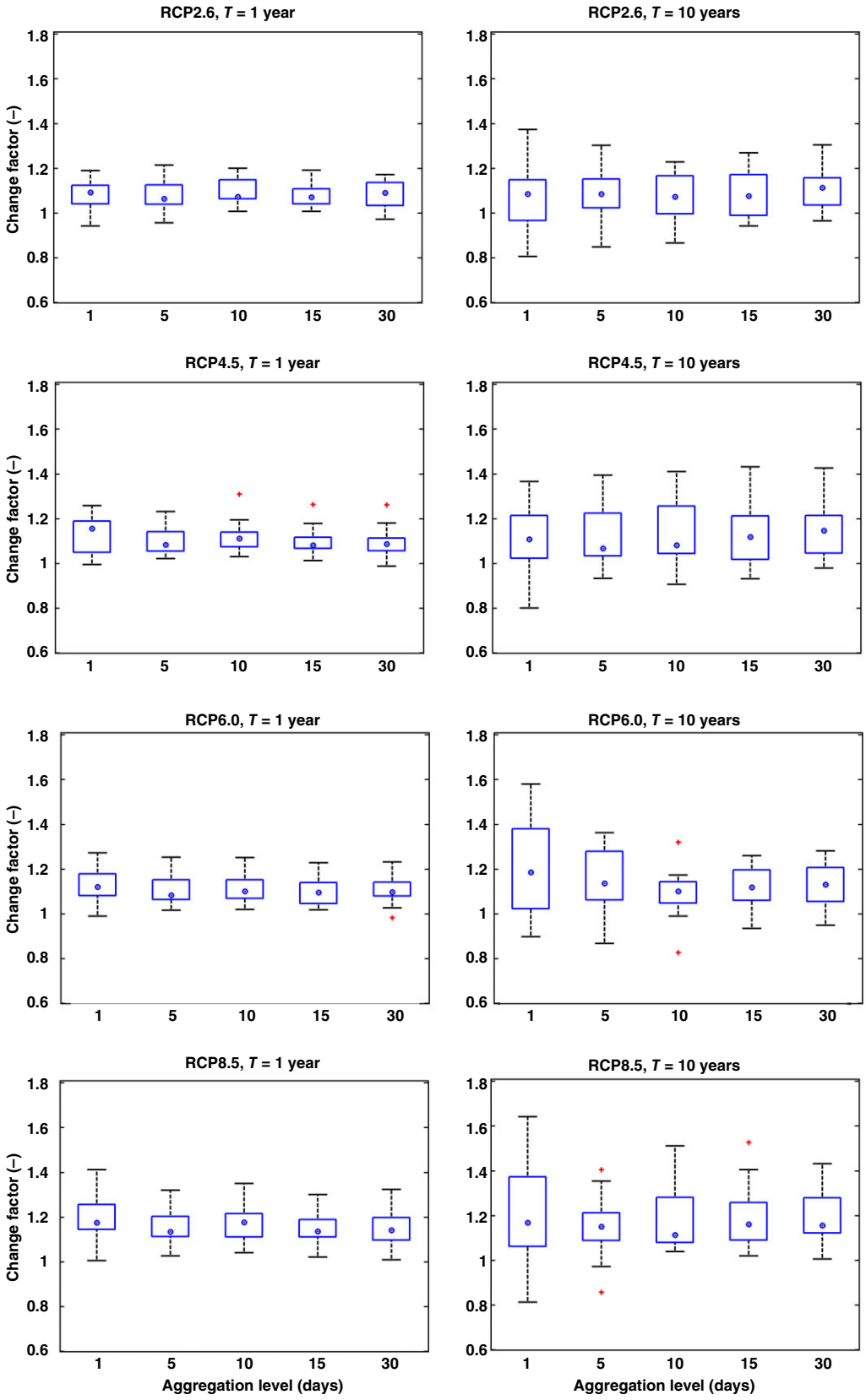

Figure 2. Change factors (from 1961–1990 to 2071–2100) for precipitation IDF statistics of different return periods and aggregation levels, and for different RCPs (top and bottom of the box show the 75th and 25th percentiles of change factors, respectively; top and bottom of the whiskers show the 5th and 95th percentiles, respectively; blue dot and red cross represent the median and outliers, respectively).

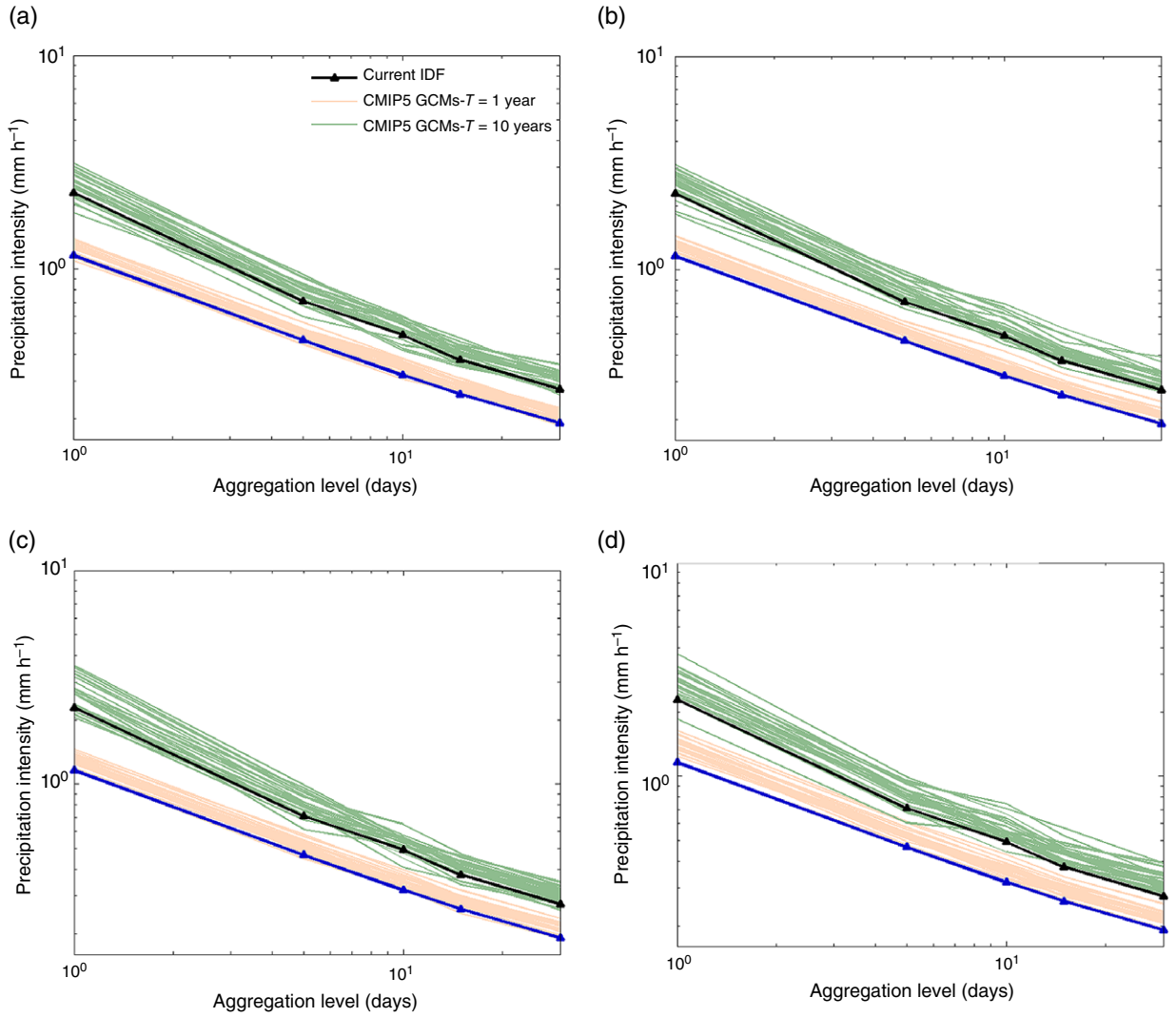

Figure 3. Future IDF curves (2071–2100) after quantile perturbation based on the CMIP5 GCMs for different RCPs versus the existing IDF curves (1961–1990) at Uccle station (observation lines for the 1- and 10-year return periods are shown in blue and black colours, respectively). (a) RCP2.6, (b) RCP4.5, (c) RCP6.0 and (d) RCP8.5.

high as 65%. This large GCM uncertainty is in agreement with the results reported in the literature (Minville *et al.*, 2008; Chen *et al.*, 2011; Hawkins and Sutton, 2011; Solaiman and Simonovic, 2011; Alam and Elshorbagy, 2015). Although GCM is the major contributor to the total uncertainty, GCM initial condition and RCP are also important. The relative contribution of the latter uncertainty sources depends on the return period and duration. The fractional contribution of each source is indeed subject to estimation uncertainties due to the limited sample size, as can be noticed by the non-monotonous changes in the contributions from low to higher return periods or from small to longer durations. General tendencies in the results show that the GCM initial condition uncertainty has a contribution percentage between 16 and 38%. The importance of GCM initial condition uncertainty has also been underlined by many climate change studies (Hawkins and Sutton, 2011; Deser *et al.*, 2012, 2014; Peel *et al.*, 2015). The RCP uncertainty ranges between 10 and 23%. This is surprisingly low, if one takes into account that the greenhouse gas concentrations are the forces driving the simulated climate changes, but consistent with the findings by other researchers (Chen *et al.*, 2011; Hawkins and Sutton, 2011; Werner, 2011; Bürger *et al.*, 2012). For all uncertainty sources, the absolute magnitude of uncertainty increases for increasing return period, from 1- to 10-years. However, since the rate of the increase for the GCM and GCM initial condition uncertainties is higher than that for the RCP, the relative contribution of the RCP uncertainty decreases from 1- to 10-year return period. To investigate whether the conclusions are sensitive to the method used for uncertainty definition, uncertainty was defined as the variance of change factors (Figure S2, Supporting information). When the results of the two uncertainty methods are compared, the results obtained from the scenario range method remain valid.

Because the larger uncertainty of GCM compared with the GCM initial condition and RCP uncertainties may be due to its larger sample size (15 GCMs *vs* 10 GCM initial conditions and 4 RCPs), the uncertainties of GCMs,

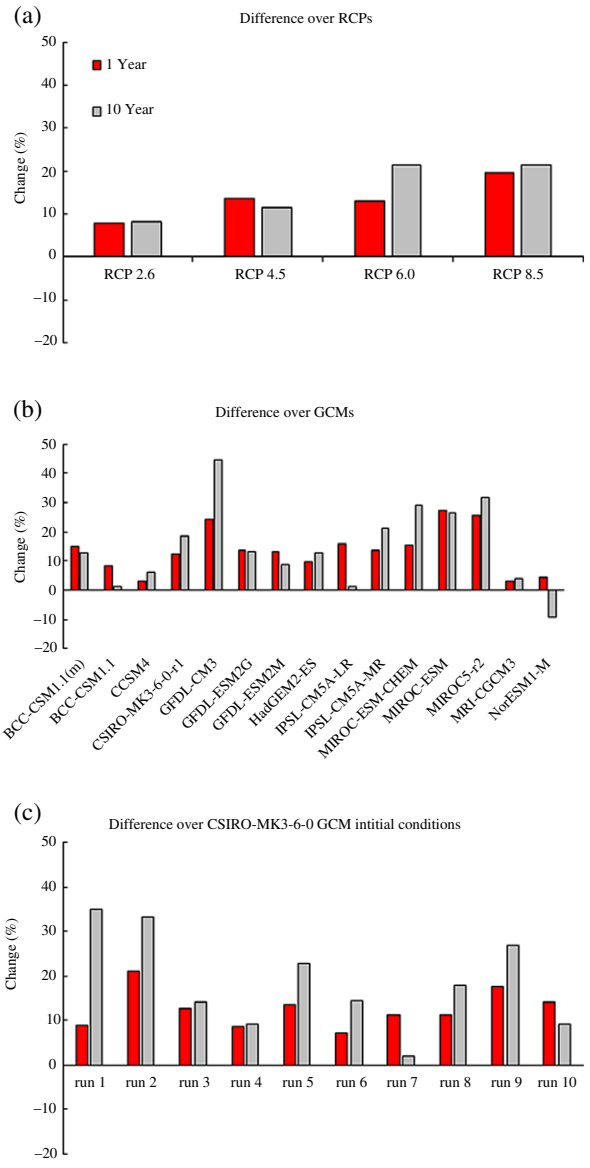

Figure 4. Changes (from 1961–1990 to 2071–2100) in daily design precipitation for different (a) RCPs, (b) GCMs and (c) GCM initial conditions. In each of the subplots, one uncertainty source is varied and the changes for the other two uncertainty sources are averaged.

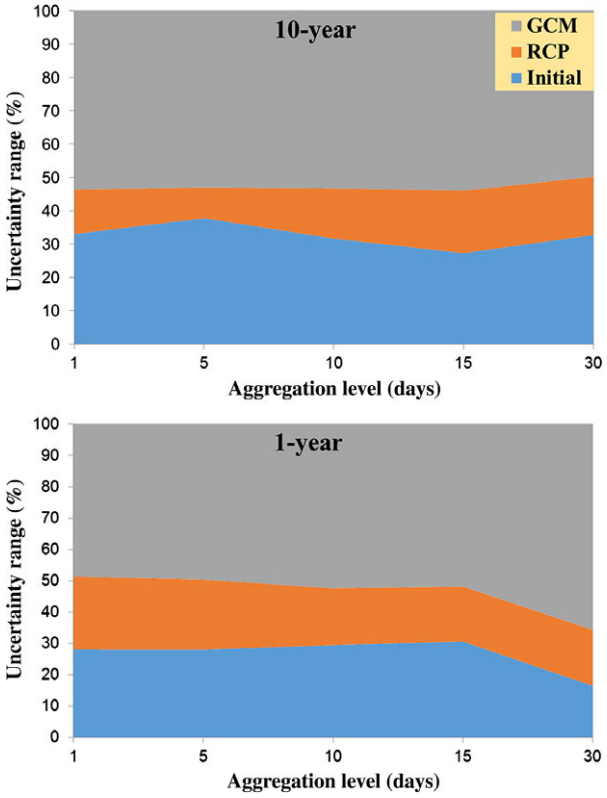

Figure 5. Percentage of total variation in change factors for design precipitation amounts explained by GCMs, RCP scenarios and GCM initial conditions uncertainties (uncertainty is defined as the scenario range of change factors).

GCM initial conditions and RCPs with the same sample size (i.e. four members) are compared (Figure 6). The results show that the GCM uncertainty is still the main source of uncertainty, albeit its magnitude decreased after decreasing its sample size. Sensitivity of the uncertainty magnitude to sample size is further investigated next.

For the GCM uncertainty, our ensemble consists of 15 GCMs and for each GCM, one control run and four scenario runs (the four RCPs) are considered, hence 75 runs in total. To investigate the influence of the number of GCM runs on the GCM uncertainty, smaller sample sizes (with random selection) with varying number of GCM members between 14 and 4 are created. Afterwards, the GCM uncertainty from these new ensembles is compared with that from the original ensemble with 15 GCMs (Figure 7). The results show that the bigger the GCM ensemble size is, the larger uncertainty will be. However, median of change factors remains more or less same among the GCM ensembles with different sample sizes. It implies that in climate change studies the mean climate scenario (median of projected changes) can be constructed based on the results of few GCMs. However, one has to be careful in constructing the high and low climate scenarios and for analyzing uncertainty using few GCMs, as the results are expected to be different from those achieved from a larger ensemble of GCMs. This is due to the fact that at such ensemble size (population size=15), the upper and lower limits of the 95% confidence interval are equal to the maximum and minimum values (15×0.025 for the upper limit and 15×0.975 for the lower limit) which are very sensitive to sample size. However, for very large size of GCM ensemble (e.g., population=100 or 200) at which the upper and lower limits of the 95% confidence level are not equal to the maximum and minimum values, median of uncertainties (high climate scenario minus low climate scenario) remains more or less the same when changing the size of ensemble (see Figure S2). The analysis is also done for the GCM initial condition uncertainty and similar results are obtained: decreasing uncertainty with decreasing sample size and a constant median of changes for different sample sizes (Figure 8).

The sensitivity analysis of the RCP uncertainty results to the sample size is also performed. In the case of future

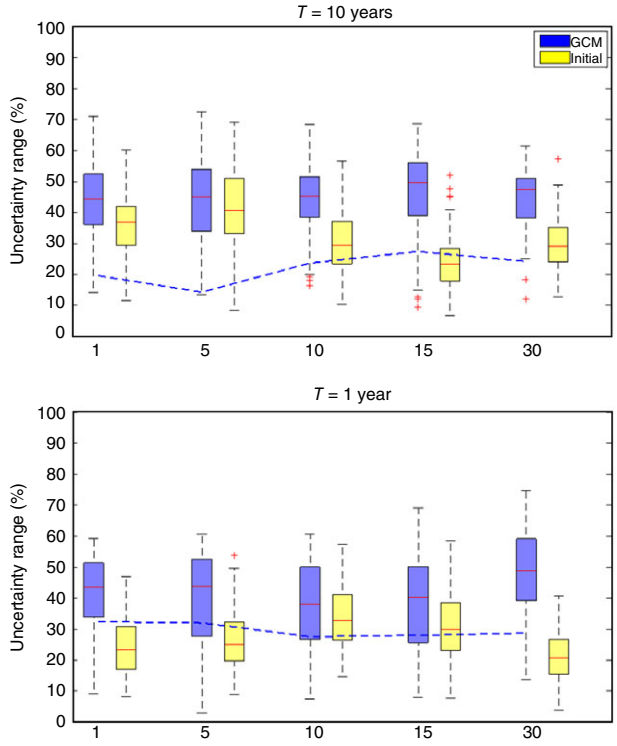

Figure 6. GCM and GCM initial condition uncertainties using the same sample size (four members) as RCPs for design precipitation changes (four GCMs or CSIRO-Mk3.6.0 runs are randomly selected from the 15 GCMs or the 10 CSIRO-Mk3.6.0 runs and this is repeated a large number of times; GCM and GCM initial condition uncertainties are shown in blue and yellow boxes, respectively; RCP uncertainty is shown with blue dashed line; top and bottom of the box show the 75th and 25th percentiles of uncertainty range, respectively; top and bottom of the whiskers show the 5th and 95th percentiles, respectively; horizontal red line in the middle of the box and red cross represent the median and outliers, respectively).

concentration scenarios, this study made use of the precipitation simulations for all four RCP scenarios (RCP2.6, RCP4.5, RCP6.0, RCP8.5). However, all RCPs have not been mostly considered in hydrological impact studies of climate change (Booth *et al.*, 2013; Mohammeda *et al.*, 2015; Fatichi *et al.*, 2016; Mandal *et al.*, 2016; Monjo *et al.*, 2016) and for simplifying and based on the research purpose, the climate model outputs for only one RCP (RCP8.5 representing the extreme future conditions or RCP4.5 representing the medium future conditions) or two RCPs (RCP4.5 & RCP8.5) have been used. From uncertainty analysis point of view, all RCPs are needed to cover the total ensemble uncertainty of climate change. Although considering RCP2.6 and RCP8.5 as the lower and upper limits of projected concentrations approximately covers this range (Hosseinzadehtalaei *et al.*, 2016); however, considering only RCP4.5 and RCP8.5 might underestimate the total uncertainty. This issue is investigated in this study by comparing the RCP uncertainty derived from 2-RCP cases (RCP2.6 & RCP8.5, RCP4.5 & RCP8.5 and RCP6.0 & RCP8.5) with that from the 4-RCP case (RCP2.6, RCP4.5, RCP6.0, RCP8.5). The results indicate that the use of extreme scenarios (RCP2.6 & RCP8.5) covers the total uncertainty range in extreme precipitation change for almost all cases, while the use of RCP4.5 & RCP8.5 and RCP6.0 & RCP8.5 will underestimate the full uncertainty (Figure 9). Similar to the GCM uncertainty, the RCP uncertainty is more sensitive to the number of runs for more extreme events and smaller time scales.

To assess the uncertainty in the initial conditions, we used 50 runs of the CSIRO-Mk3.6.0 GCM (10 runs for the control period and 40 runs for the four RCPs). Such high numbers of GCM/RCM members are rarely available in climate model ensembles; the number of runs per GCM and RCP combination in the CMIP5 ensemble (as the largest ensemble available) is still of the order of 3–10. Due to this lack of available runs per GCM, a limited number of runs have been used for initial condition uncertainty in climate change impact assessments, e.g. five runs of a GCM in Chen *et al.* (2011) and five and three runs for two GCMs in Velázquez *et al.* (2013). Despite the high number of runs available for the CSIRO-Mk3.6.0 model, the fractional uncertainty related to the GCM initial conditions in Figure 5 was related to that single GCM only. A critical question here is how much the uncertainty associated to the GCM initial conditions will change when choosing another GCM instead of the CSIRO-Mk3.6.0 model. To answer this research question, the initial condition uncertainty is reperformed using the simulations of the HadGEM2-ES, CCSM4 GCMs and CSIRO-Mk3.6.0 with 3 runs (i.e. different initial conditions) for each control and four RCPs periods (that makes the total runs of this GCM equal to 15). A comparison of uncertainty ranges for GCM initial conditions using the same number of runs (i.e. 3 runs) for the three GCMs is presented in Figure 10. For daily precipitation of 10-year return period, the CCSM4 model has the largest uncertainty range, while the CSIRO-Mk3.6.0 model shows the largest uncertainty for five-daily precipitation of the same return period. Apart from more extreme precipitation at smaller time scales, the difference between the uncertainty range for different GCMs is negligible.

4. Concluding remarks

In the current study, future changes in intense precipitation and IDF relationships for Belgium and associated uncertainties were quantified by using a large ensemble of projections gained from 15 GCMs under four RCPs (RCP2.6, RCP4.5, RCP6.0 and RCP8.5) for different return periods and durations. The results indicate an amplification in the intensity of precipitation extremes for the end of the 21st century relative to the current climate. The amount of increase varies depending on the GCMs, RCPs and GCM initial conditions and can go up to around 64%. The uncertainty analysis shows that the choice and set of GCMs is the largest source of uncertainty for all the return periods and aggregation levels considered. However, the other sources of uncertainties cannot be neglected and need to be taken into account as well, as for some cases fractional uncertainties of up to 38 and 23% are observed for GCM initial conditions and RCPs, respectively. This quantification of uncertainties in future IDF

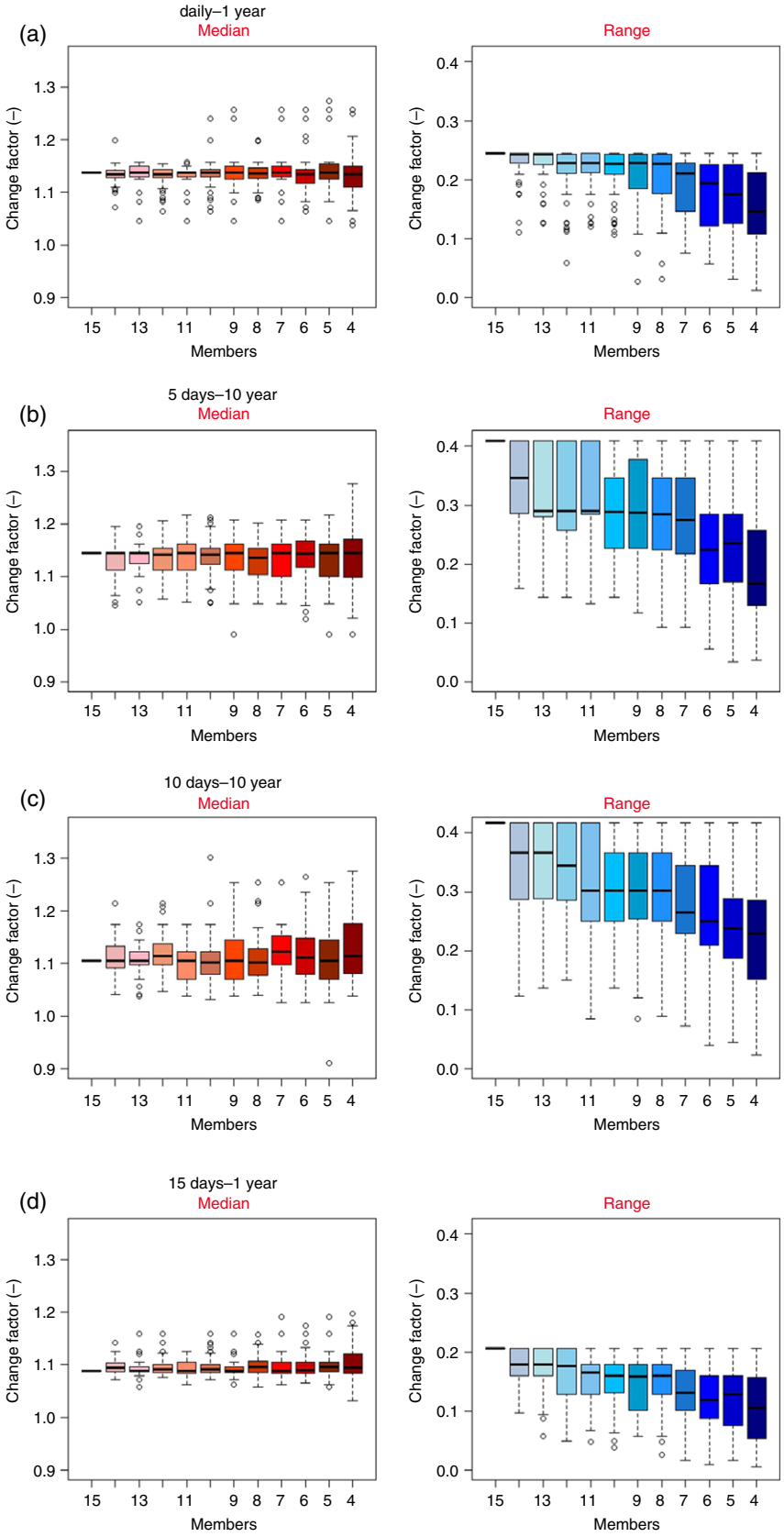

Figure 7. Comparison of (a)–(d) median and range of change factors for different GCM ensemble sizes (smaller sample sizes are randomly selected from the 15 GCMs and this is repeated a large number of times; uncertainty range is computed as the difference between the high and low climate scenarios defined based on the 95% confidence intervals; top and bottom of the box show the 75th and 25th percentiles of change factors, respectively; top and bottom of the whiskers show the 5th and 95th percentiles, respectively; horizontal black line in the middle of the box and hollow black dot represent the median and outliers, respectively).

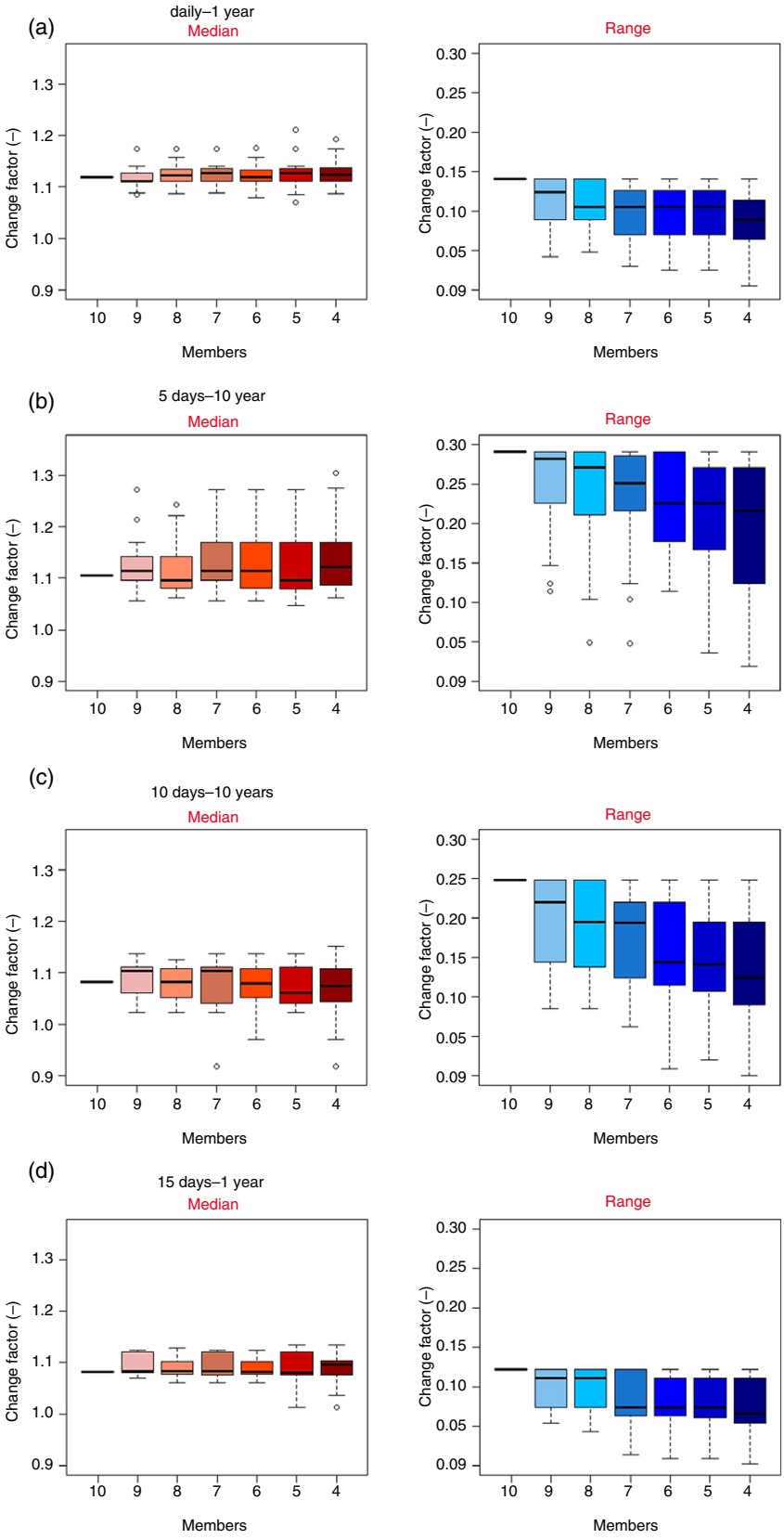

Figure 8. Comparison of (a)–(d) median and range of change factors for GCM initial conditions with different number of runs (smaller sample sizes are randomly selected from the 10 GCM initial conditions and this is repeated a large number of times; Uncertainty range is computed as the difference between the high and low climate scenarios defined based on the 95% confidence intervals; top and bottom of the box show the 75th and 25th percentiles of change factors, respectively; top and bottom of the whiskers show the 5th and 95th percentiles, respectively; horizontal black line in the middle of the box and hollow black dot represent the median and outliers, respectively).

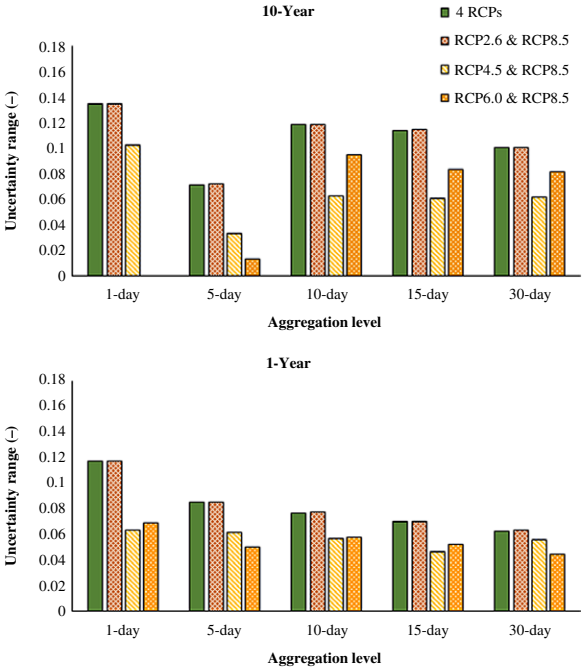

Figure 9. Comparison of uncertainty ranges considering four and two RCPs (uncertainty range is computed as the difference between the high and low climate scenarios defined based on the 95% confidence intervals).

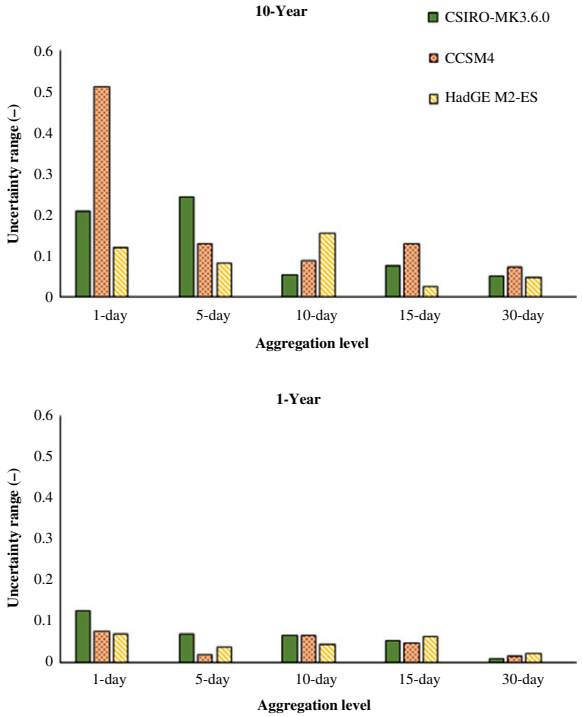

Figure 10. Comparison of uncertainty ranges for GCM initial conditions for different GCMs with the same number of runs (uncertainty range is computed as the difference between the high and low climate scenarios defined based on the 95% confidence intervals).

curves represents useful information for hydraulic and water engineering design and modelling, as well as impact and adaptation studies. It is also found from the sensitivity analysis that the uncertainties in the GCMs, RCPs and GCM initial conditions are sensitive to the size of climate model ensemble, particularly in the case of more intense precipitation at smaller temporal resolution.

Generally, there is no practical method to identify the optimal size of a climate model ensemble. Although some approaches based on climate model performance for the present-day climate and giving corresponding weight to them [e.g. reliability ensemble average (REA) method by Giorgi and Mearns, 2002] have been developed for optimizing climate model projections for the future, better skill of a climate model for present-day climate simulations does not guarantee the validity of its future projections (Tebaldi and Knutti, 2007). However, with regard to quantification of all aspects of uncertainty in future climate change in a probabilistic way, a large multi-model ensemble is needed. In addition, including more independent climate models boosts our confidence on climate change projections for the future, since combining the outputs of several individual models will lead to better ability and higher reliability of projections for the highly complex climate system. This is the case for the ensembles at which climate models are less homogeneous in the sense of the climate processes they include or neglect and in their structure.

The results of this study highlight the importance of ensemble size for the uncertainty analysis of climate change. The increase in the climate model ensemble size to cover the full uncertainty in climate change projections and the improvement of model accuracy (e.g. increasing model resolution) to present a more realistic simulation of the climate system are two competing demands for climate modelling centres. These are two important issues for climate change impact assessments and neither should be sacrificed for another and there must be a balance between them based on available computational resources.

In this study, the sensitivity of climate change uncertainty to the number of GCM runs was analysed, assuming that the GCMs in the multi-model ensemble provide statistically independent information. However, some factors may affect the validity of this assumption since some GCMs are developed in the same climate modelling centre or they are developed in different centres but may share some part of the code or use the same theoretical arguments for parameterizations (Sunyer *et al.*, 2013b). The assumption of model independence hence needs further investigation.

Acknowledgements

The authors acknowledge the World Climate Research Programme's Working Group on Coupled Modelling – phase 5 (CMIP5), and the climate modelling centres involved in that programme. The work has been funded by projects for the Belgian Science Policy Office (CORDEX.be), the Flemish Environment Agency, and the European Union's Horizon 2020 research and innovation programmes under grant agreement No 700699, project BRIGAID (BRIdges the GAp for Innovations in Disaster

resilience), and grant agreement No 730004, project PUCS (Pan-European Urban Climate Service).

Supporting information

The following supporting information is available as part of the online article:

Figure S1. Percentage of total variation in change factors for design precipitation amounts explained by GCMs, RCP scenarios and GCM initial conditions' uncertainties (uncertainty is defined as the variance of change factors).

Figure S2. Comparison of median (left column) and range (right column) in the ensembles with different sample sizes (population consists of 200 randomly produced numbers with similar value range to precipitation change factors; smaller sample sizes are randomly selected from the population and this is repeated a large number of times; top and bottom of the box show the 75th and 25th percentiles of randomly generated values, respectively; top and bottom of the whiskers show the 5th and 95th percentiles, respectively; horizontal black line in the middle of the box represents the median).

References

Ahmed KF, Wang G, Silander J, Wilson AM, Allen JM, Horton R, Anyah R. 2013. Statistical downscaling and bias correction of climate model outputs for climate change impact assessment in the U.S. northeast. *Glob. Planet. Change* **100**: 320–332.

Alam MS, Elshorbagy A. 2015. Quantification of the climate change-induced variations in intensity–duration–frequency curves in the Canadian Prairies. *J. Hydrol.* **527**: 990–1005.

Alfieri L, Burek P, Feyen L, Forzieri G. 2015. Global warming increases the frequency of river floods in Europe. *Hydrol. Earth Syst. Sci.* **19**: 2247–2260.

Booth BBB, Bernie D, McNeall D, Hawkins E, Caesar J, Boulton C, Friedlingstein P, Sexton DMH. 2013. Scenario and modelling uncertainty in global mean temperature change derived from emission-driven global climate models. *Earth Syst. Dyn.* **4**(1): 95–108.

Brekke L, Barsugli J. 2013. Uncertainties in projections of future changes in extremes. In *Extremes in a Changing Climate: Detection, Analysis and Uncertainty*, AghaKouchak A, Easterling D, Hsu K, Schubert S, Sorooshian S (eds). Springer: Dordrecht, The Netherlands, 309–346.

Bürger G, Sobie SR, Cannon AJ, Werner AT, Murdock TQ. 2012. Downscaling extremes: an intercomparison of multiple methods for future climate. *J. Clim.* **26**: 3429–3449.

Cannon AJ. 2015. Selecting GCM scenarios that span the range of changes in a multimodel ensemble: application to CMIP5 climate extremes indices. *J. Clim.* **28**(3): 1260–1267.

Cannon AJ, Sobie SR, Murdock TQ. 2015. Bias correction of GCM precipitation by quantile mapping: how well do methods preserve changes in quantiles and extremes? *J. Clim.* **28**: 6938–6959.

Chen J, Brissette FP, Poulin A, Leconte R. 2011. Overall uncertainty study of the hydrological impacts of climate change for a Canadian watershed. *Water Resour. Res.* **47**(12), doi: 10.1029/2011WR010602.

Chen H, Sun J, Chen X. 2014. Projection and uncertainty analysis of global precipitation-related extremes using CMIP5 models. *Int. J. Climatol.* **34**: 2730–2748.

Cheng L, AghaKouchak A. 2014. Precipitation intensity-duration-frequency curves for infrastructure design in a changing climate. *Sci. Rep.* **4**, doi: 10.1038/srep07093.

De Paola F, Giugni M, Topa ME, Bucchignani E. 2014. Intensity-Duration-Frequency (IDF) rainfall curves, for data series and climate projection in African cities. *Springer Plus* **3**(1), doi: 10.1186/2193-1801-3-133.

Deser C, Phillips A, Bourdette V, Teng H. 2012. Uncertainty in climate change projections: the role of internal variability. *Clim. Dyn.* **38**: 527–546.

Deser C, Phillips AS, Alexander MA, Smoliak BV. 2014. Projecting North American climate over the next 50 years: uncertainty due to internal variability. *J. Clim.* **27**: 2271–2296.

Dessu SB, Melesse AM. 2013. Impact and uncertainties of climate change on the hydrology of the Mara River basin, Kenya/Tanzania. *Hydrol. Process.* **27**(20): 2973–2986.

Fatichi S, Ivanov VY, Paschalis A, Peleg N, Molnar P, Rimkus S, Kim J, Burlando P, Caporali E. 2016. Uncertainty partition challenges the predictability of vital details of climate change. *Earth's Future* **4**(5): 240–251.

Ferro CA, Jupp TE, Lambert FH, Huntingford C, Cox PM. 2012. Model complexity versus ensemble size: allocating resources for climate prediction. *Philos. Trans. R. Soc. A. Math. Phys. Eng. Sci.* **370**(1962): 1087–1099.

Giorgi F, Mearns LO. 2002. Calculation of average, uncertainty range, and reliability of regional climate changes from AOGCM simulations via the "reliability ensemble averaging" (REA) method. *J. Clim.* **15**: 1141–1158.

Hawkins E, Sutton R. 2009. The potential to narrow uncertainty in regional climate predictions. *Bull. Am. Meteorol. Soc.* **90**: 1095–1107.

Hawkins E, Sutton R. 2011. The potential to narrow uncertainty in projections of regional precipitation change. *Clim. Dyn.* **37**(1–2): 407–418.

Haylock MR, Hofstra N, Klein Tank AMG, Klok EJ, Jones PD, New M. 2008. A European daily high-resolution gridded dataset of surface temperature and precipitation. *J. Geophys. Res. Atmos.* **113**: D20119.

Horton RM, Coffel ED, Winter JM, Bader DA. 2015. Projected changes in extreme temperature events based on the NARCCAP model suite. *Geophys. Res. Lett.* **42**: 7722–7731.

Hosseinzadehtalaei P, Tabari H, Willems P. 2016. Quantification of uncertainty in reference evapotranspiration climate change signals in Belgium. *Hydrol. Res.* , doi: 10.2166/nh.2016.243.

Hughes DA, Kingston DG, Todd MC. 2011. Uncertainty in water resources availability in the Okavango River basin as a result of climate change. *Hydrol. Earth Syst. Sci.* **15**: 931–941.

IPCC. 2012. Managing the risks of extreme events and disasters to advance climate change adaptation. In *A Special Report of Working Groups I and II of the Intergovernmental Panel on Climate Change*, Field CB, Barros V, Stocker TF, Qin D, Dokken DJ, Ebi KL, Mastrandrea MD, Mach KJ, Plattner G-K, Allen SK, Tignor M, Midgley PM (eds.). Cambridge University Press: New York.

IPCC. 2013. Summary for policymakers. In *Climate Change 2013. The Physical Science Basis, Contribution of Working Group I to the Fifth Assessment Report of the Intergovernmental Panel on Climate Change*, Stocker TF, Qin D, Plattner GK, Tignor M, Allen SK, Boschung J, Nauels A, Xia Y, Bex V, Midgley PM (eds). IPCC: Geneva, Switzerland, 1–27.

Janssen E, Sriver RL, Wuebbles DJ, Kunkel KE. 2016. Seasonal and regional variations in extreme precipitation event frequency using CMIP5. *Geophys. Res. Lett.* **43**: 5385–5393, doi: 10.1002/2016GL069151.

Kharin V, Zwiers F, Zhang X, Wehner M. 2013. Changes in temperature and precipitation extremes in the CMIP5 ensemble. *Clim. Change* **119**: 345–357.

Kim BS, Jeung SJ, Lee DS, Han WS. 2015. Nonstationary intensity-duration-frequency curves for drainge infrastructure coping with climate change. In *EGU General Assembly Conference Abstracts*, 17, p. 8349.

Kingston DG, Thompson JR, Kite G. 2011. Uncertainty in climate change projections of discharge for the Mekong River Basin. *Hydrol. Earth Syst. Sci.* **15**: 1459–1471.

Knutti R, Sedláček J. 2013. Robustness and uncertainties in the new CMIP5 climate model projections. *Nat. Clim. Change* **3**(4): 369–373.

Latifa A, Yousef Taha BMJ, Ouarda . 2015. Adaptation of water resources management to changing climate: the role of intensity-duration-frequency curves. *Int. J. Environ. Sci. Dev.* **6**(6): 478–483.

Liepert BG, Previdi M. 2012. Inter-model variability and biases of the global water cycle in CMIP3 coupled climate models. *Environ. Res. Lett.* **7**: 014006.

Liew SC, Srivatsan VR, Liong SH. 2014. Development of intensity-duration-frequency curves at ungauged sites: risk management under changing climate. *Geosci. Lett.* **1**: 8, doi: 10.1186/2196-4092-1-8.

Liu Z, Mehran A, Phillips TJ, AghaKouchak A. 2014. Seasonal and regional biases in CMIP5 precipitation simulations. *Clim. Res.* **60**(1): 35–50.

Lutz AF, ter Maat HW, Biemans H, Shrestha AB, Wester P, Immerzeel WW. 2016. Selecting representative climate models for climate

change impact studies: an advanced envelope-based selection approach. *Int. J. Climatol.* **36**: 3988–4005.
Madsen H, Arnbjerg-Nielsen K, Mikkelsen PS. 2009. Update of regional intensity-duration-frequency curves in Denmark: tendency towards increased storm intensities. *Atmos. Res.* **92**(3): 343–349.
Mailhot A, Duchesne S, Caya D, Talbot G. 2007. Assessment of future change in intensity-duration-frequency (IDF) curves for Southern Quebec using the Canadian Regional Climate Model (CRCM). *J. Hydrol.* **347**: 197–210.
Mandal S, Breach PA, Simonovic SP. 2016. Uncertainty in precipitation projection under changing climate conditions: a regional case study. *Am. J. Clim. Change* **5**(01): 116.
Maraun D. 2016. Bias correcting climate change simulations – a critical review. *Curr. Clim. Change Rep.* **2**: 211–220.
Maurer EP, Pierce DW. 2014. Bias correction can modify climate model simulated precipitation changes without adverse effect on the ensemble mean. *Hydrol. Earth Syst. Sci.* **18**: 915–925.
Meehl G, Bony S. 2011. Introduction to CMIP5. *CLIVAR Exchanges* **16**: 4–5.
Mendlik T, Gobiet A. 2016. Selecting climate simulations for impact studies based on multivariate patterns of climate change. *Clim. Change* **135**: 381–393.
Min SK, Simonis D, Hense A. 2007. Probabilistic climate change predictions applying Bayesian model averaging. *Philos. Trans. R. Soc. A Math. Phys. Eng. Sci.* **365**: 2103–2116.
Minville M, Brissette F, Leconte R. 2008. Uncertainty of the impact of climate change on the hydrology of a nordic watershed. *J. Hydrol.* **358**: 70–83.
Modesto Gonzalez Pereira MJ, Sanches Fernandes LF, Barros Macário EM, Gaspar SM, Pinto JG. 2014. Climate change impacts in the design of drainage systems: case study of Portugal. *J. Irrig. Drain. Eng.* **141**(2): 05014009.
Mohammeda IN, Arne Bomblies A, Wemplea BC. 2015. The use of CMIP5 data to simulate climate change impacts on flow regime within the Lake Champlain Basin. *J. Hydrol. Reg. Stud.* **3**: 160–186.
Monjo R, Gaitán E, Pórtoles J, Ribalaygua J, Torres L. 2016. Changes in extreme precipitation over Spain using statistical downscaling of CMIP5 projections. *Int. J. Climatol.* **36**: 757–769.
Ning L, Bradley RS. 2016. NAO and PNA influences on winter temperature and precipitation over the eastern United States in CMIP5 GCMs. *Clim. Dyn.* **46**: 1257–1276.
Ning L, Riddle EE, Bradley RS. 2015. Projected changes in climate extremes over the northeastern United States. *J. Clim.* **28**: 3289–3310.
Ntegeka V, Baguis P, Roulin E, Willems P. 2014. Developing tailored climate change scenarios for hydrological impact assessments. *J. Hydrol.* **508C**: 307–321.
O'Gorman PA. 2015. Precipitation extremes under climate change. *Curr. Clim. Change Rep.* **1**(2): 49–59.
Panday PK, Thibeault J, Frey KE. 2015. Changing temperature and precipitation extremes in the Hindu Kush-Himalayan region: an analysis of CMIP3 and CMIP5 simulations and projections. *Int. J. Climatol.* **35**: 3058–3077.
Peck A, Prodanovic P, Simonovic SPP. 2012. Rainfall intensity duration frequency curves under climate change: city of London, Ontario, Canada. *Can. Water Resour. J.* **37**(3): 177–189.
Peel MC, Srikanthan R, McMahon TA, Karoly DJ. 2015. Approximating uncertainty of annual runoff and reservoir yield using stochastic replicates of global climate model data. *Hydrol. Earth Syst. Sci.* **19**(4): 1615–1639.
Rana A, Foster K, Bosshard T, Olsson J, Bengtsson L. 2014. Impact of climate change on rainfall over Mumbai using Distribution-based scaling of global climate model projections. *J. Hydrol. Reg. Stud.* **1**: 107–128.
Randall DA, RA Wood RA, Bony S, Colman R, Fichefet T, Fyfe J, Kattsov V, Pitman A, Shukla J, Srinivasan J, Stouffer RJ, Sumi A, Taylor KE. 2007. Climate models and their evaluation. In *Climate Change 2007: The Physical Science Basis. Contribution of Working Group I to the Fourth Assessment Report of the Intergovernmental Panel on Climate Change*, Solomon S, Qin D, Manning M, Chen Z, Marquis M, Averyt KB, Tignor M, Miller HL (eds). Cambridge University Press: Cambridge, UK; New York, NY.
Sierra JP, Arias PA, Vieira SC. 2015. Precipitation over northern South America and its seasonal variability as simulated by the CMIP5 models. *Adv. Meteorol.* **2015**: 1–22.
Sillmann J, Kharin VV, Zhang X, Zwiers FW, Bronaugh D. 2013a. Climate extremes indices in the CMIP5 multimodel ensemble: part 1. Model evaluation in the present climate. *J. Geophys. Res. Atmos.* **118**: 1716–1733.
Sillmann J, Kharin VV, Zwiers FW, Zhang X, Bronaugh D. 2013b. Climate extremes indices in the CMIP5 multimodel ensemble: part 2. Future climate projections. *J. Geophys. Res. Atmos.* **118**: 2473–2493.
Solaiman TA, Simonovic SP. 2011. Development of probability based intensity-duration-frequency curves under climate change. Water Resource Research Report No. 072, Facility for Intelligent Decision Support, Department of Civil and Environmental Engineering, London, Ontario, Canada.
Strobach E, Bel G. 2015. The contribution of internal and model variabilities to the uncertainty in CMIP5 decadal climate predictions. arXiv preprint arXiv:1508.01609.
Sunyer MA, Madsen H, Rosbjerg D, Arnbjerg-Nielsen K. 2013a. Regional interdependency of precipitation indices across Denmark in two ensembles of high-resolution RCMs. *J. Clim.* **26**(20): 7912–7928.
Sunyer MA, Sørup HJD, Christensen OB, Madsen H, Rosbjerg D, Mikkelsen PS, Arnbjerg-Nielsen K. 2013b. On the importance of observational data properties when assessing regional climate model performance of extreme precipitation. *Hydrol. Earth Syst. Sci.* **17**(11): 4323–4337.
Sunyer MA, Gregersen IB, Rosbjerg D, Madsen H, Luchner J, Arnbjerg-Nielsen K. 2015. Comparison of different statistical downscaling methods to estimate changes in hourly extreme precipitation using RCM projections from ENSEMBLES. *Int. J. Climatol.* **35**: 2528–2539.
Tabari H, Taye MT, Willems P. 2015. Water availability change in central Belgium for the late 21st century. *Glob. Planet. Change* **131**: 115–123.
Tabari H, De Troch R, Giot O, Hamdi R, Termonia P, Saeed S, Brisson E, Van Lipzig N, Willems P. 2016a. Local impact analysis of climate change on precipitation extremes: are high-resolution climate models needed for realistic simulations? *Hydrol. Earth Syst. Sci.* **20**: 3843–3857.
Tabari H, Hosseinzadehtalaei P, Willems P, Saeed S, Brisson E, Van Lipzig N. 2016b. How will be future rainfall IDF curves in the context of climate change? In *Proceedings of the 4th IAHR Europe Congress*, Liege, Belgium, 27–29 July 2016.
Taylor KE, Stouffer RJ, Meehl GA. 2012. An overview of CMIP5 and the experiment design. *Bull. Am. Meteorol. Soc.* **93**: 485–498.
Tebaldi C, Knutti R. 2007. The use of the multi-model ensemble in probabilistic climate projections. *Philos. Trans. R. Soc. A Math. Phys. Eng. Sci.* **365**(1857): 2053–2075.
Velázquez JA, Schmid J, Ricard S, Muerth MJ, Gauvin St-Denis B, Minville M, Chaumont D, Caya D, Ludwig R, Turcotte R. 2013. An ensemble approach to assess hydrological models' contribution to uncertainties in the analysis of climate change impact on water resources. *Hydrol. Earth Syst. Sci.* **17**: 565–578.
Werner AT. 2011. BCSD downscaled transient climate projections for eight select GCMs over British Columbia, Canada. Hydrologic Modelling Project Final Report (Part I), 63 pp.
Willems P. 2000. Compound intensity/duration/frequency-relationships of extreme precipitation for two seasons and two storm types. *J. Hydrol.* **233**: 189–205.
Willems P. 2013. Revision of urban drainage design rules after assessment of climate change impacts on precipitation extremes at Uccle, Belgium. *J. Hydrol.* **496**: 166–177.
Willems P, Vrac M. 2011. Statistical precipitation downscaling for small-scale hydrological impact investigations of climate change. *J. Hydrol.* **402**: 193–205.
Willems P, Arnbjerg-Nielsen K, Olsson J, Nguyen VTV. 2012a. Climate change impact assessment on urban rainfall extremes and urban drainage: methods and shortcomings. *Atmos. Res.* **103**: 106–118.
Willems P, Olsson J, Arnbjerg-Nielsen K, Beecham S, Pathirana A, Gregersen IB, Madsen H, Nguyen VTV. 2012b. *Impacts of Climate Change on Rainfall Extremes and Urban Drainage*. IWA Publishing: London.
Wu CH, Huang GR, Yu HJ. 2015. Prediction of extreme floods based on CMIP5 climate models: a case study in the Beijiang River basin, South China. *Hydrol. Earth Syst. Sci.* **19**: 1385–1399, doi: 10.5194/hess-19-1385-2015.
Yilmaz AG, Hossain I, Perera BJC. 2014. Effect of climate change and variability on extreme rainfall intensity–frequency–duration relationships: a case study of Melbourne. *Hydrol. Earth Syst. Sci.* **18**: 4065–4076, doi: 10.5194/hess-18-4065.
Yin L, Fu R, Shevliakova E, Dickinson RE. 2013. How well can CMIP5 simulate precipitation and its controlling processes over tropical South America? *Clim. Dyn.* **41**: 3127, doi: 10.1007/s00382-012-1582-y.

